Imaging of Cerebrospinal Fluid Space and Movement of Hydrocephalus Mice using Near Infrared Fluorescence

YASUSHI SHIBATA, M.D., PH.D.,

JONATHAN B. KRUSKAL, M.D., PH.D., MATTHEW R. PALMER, PH.D.

Department of Radiology, Beth Israel Deaconess Medical Center,

330 Brookline Ave. Boston, MA, 02215, USA

Address for correspondence and reprint request:

Yasushi Shibata, M.D., Ph.D.

Department of Neurosurgery, Institute of Clinical Medicine, University of Tsukuba,

Tsukuba, Ibaraki, 305-8575, Japan

Tel; +81-298-53-3220

Fax; +81-298-53-3214

E-mail; yshibata@md.tsukuba.ac.jp

Acknowledgement

This study was financially supported by Radiology Foundation Research Award from Department of Radiology, Beth Israel Deaconess Medical Center (to Y.S.).

Abstract

Introduction: We have studied optical imaging of mice cerebrospinal fluid (CSF) space and flow using near infrared fluorescence. We applied our method to image CSF space and flow in a mice hydrocephalus model. Material and Methods: Hydrocephalus was induced in mice with intracranial injections of transforming growth factor. Hydrocephalic and control mice were imaged using our near infrared fluorescence imaging system. Results: Hydrocephalic mice showed diminished intracranial CSF flow. Discussion: Our system is sufficient to show altered CSF flow in a mouse hydrocephalus model. Optical imaging using near infrared is an effective modality to image CSF space and movement.

Key words: *cerebrospinal fluid, fluorescence, hydrocephalus, mice, near infrared*

Introduction

Clinically, dynamic cerebrospinal fluid (CSF) imaging is performed using radioisotope (RI) or computed tomography (CT) cisternography or cine-mode magnetic resonance imaging (cine MRI). RI cisternography has low spatial resolution and involves the complicated handling of radioisotopic materials. CT cisternography shows axial tomographic images with high spatial resolution, however sagittal images are not possible. In addition, there is the possibility of adverse reactions induced by intrathecally injected metrizamide [1]. Both RI and CT cisternography have the disadvantage of involving exposure to ionizing radiation. Cine MRI is non-invasive and has high resolution, however the entire flow dynamics, including wash out from the CSF space, is not evaluated [2].

To overcome these limitations, we have developed an optical method of CSF space imaging and flow measurement using a novel near infrared (NIR) fluorescence imaging methodology. Previously we reported imaging of CSF space and movement using this method in normal mice [3]. The objective of this study is to employ this method to evaluate pathological CSF flow in hydrocephalic mice.

Hydrocephalus is a typical pathological CSF flow disease. In our study, communicating hydrocephalus in mice was induced by an intrathecal injection of human recombinant transforming growth factor β1 (TGF-β1). TGF-β1 injected mice are expected to exhibit ventricular dilatation within 3 weeks [4] and in this study they undergo imaging studies 4 weeks after the injection.

Material and Methods

Compounds

Indocyanine green (ICG) is a tricarbocyanine dye which, as an aqueous solution, has a major absorption peak at approximately 780 nm, a minor peak at approximately 700 nm, and fluorescent emission peak at approximately 820 nm. ICG (Sigma-Aldrich, St. Louis, MO) was prepared as 6.45mM solution in 0.8% NaCl. Human high-density lipoprotein (HDL, Sigma-Aldrich, St. Louis, MO) was prepared as 10mg/ml solution in phosphate buffered saline (PBS, Sigma-Aldrich, St. Louis, MO). Five micro liter of prepared 6.45mM ICG solution was

mixed with 0.5 ml of prepared 10 mg/ml human HDL solution because ICG is bound to lipoprotein in circulating blood [5]. Human TGF-β1 was purchased from Sigma-Aldrich (St. Louis, MO). 100 mg of Bovine serum albumin (BSA) powder (Sigma-Aldrich, St. Louis, MO) was dissolved in 100 ml of PBS. One microgram of TGF-β1 was dissolved in 1ml of PBS with 0.1% BSA.

Induction of hydrocephalus

CD-1 Nude mice were purchased from Charles River Laboratories (Wilmington, MA). Communicating hydrocephalus was induced in mice using the method of Tada et al. [3]. Mice were anesthetized with intraperitoneal injection of a mixture of ketamine (100mg/kg) and xylazine (10mg/kg) at day 10 and day 11 after birth. Then, on each day, 300 ng of TGF-β1 in 30 μl of PBS was injected into the parietal lobe using a Hamilton microsyringe (Hamilton, Reno, Nevada). Control mice were injected with 30 μl of PBS with 0.1% BSA on each day.

After the mice reached 6 weeks old, they were anesthetized by intraperitoneal injection of ketamine and xylazine. The body weight of each mouse was measured just before the injection of anesthesia. Under a stereoscopic operating microscope, the 5^{th} lumbar lamina was removed and the spinal cord covered with dura matter was exposed. Then, 5 μl of ICG-HDL mixture was injected into the spinal subarachnoid space using a Hamilton microsyringe.

Imaging hardware

Anesthetized mice were positioned in the optical imaging system developed in our laboratory. Prior to each measurement, the head and feet were carefully located at the same positions on the stage of imaging system. The system was configured for epi-fluorescence measurements at NIR wavelengths using the illumination light from a 450 W Xe arc lamp (Oriel Instruments, Stratford, CT) and narrow band excitation filtration obtained by an interference filter (Omega Optical, Andover, MA, custom order) with a bandwidth of 33 nm and central wavelength of 755 nm. Emission light was filtered with a long pass optical filter (Omega Optical) with a cutoff at 798 nm. Whole-body images were digitized by a high resolution, cooled, CCD digital camera (ORCA-ER, Hamamatsu, Hamamatsu City, Japan) attached to a Pentium III-based personal computer running Lab VIEW 6 system integration and automation software (National Instruments, Austin, TX).

Image acquisition and processing

The progress of ICG tracer was monitored by the imaging system as evidenced by the intensity of the NIR fluorescence signal emitted. Dynamic measurements of CSF movement were obtained by repeating the imaging procedure at 0.5, 1, 2, 4, 6, 24 hours post injection. In addition, some mice were imaged at 30 and 48 hours following injection of the tracer. Quantitative assessment of CSF movement was assessed by placing regions of interest on

emission images and plotting the time-intensity profiles. If we could detect a clear signal from the basal cistern, we placed ROIs at these points. If the basal cistern signal was not detectable, we put ROIs at appropriate positions using the head and ear locations as references.

All images were acquired with the lens aperture set to F/1.6 and in the full resolution (1280 X 1024 pixels), non-binning, frame blanking acquisition mode of the Hamamatsu camera. The exposure time for all images was 1.2 seconds.

Each image was acquired using Lab VIEW 6 software in PNG format. These images were processed and converted to TIFF format using custom software running on MATLAB release 12.1. (The Mathworks Inc., Natick MA). Further image manipulation, compression to 8-bit scale and annotations were performed with Photoshop 6.0 software (Adobe systems Inc., San Jose, CA) on a Pentium III-based personal computer under the Windows 2000 PC platform.

The CSF movement was investigated in hydrocephalus and control mice. A total of 11 TGF-β1 injected hydrocephalic mice and 10 PBS injected control mice were imaged. The CSF movement patterns were established and the time-intensity curves were analyzed.

Ventricle/brain ratio

After the image acquisition, every mouse was sacrificed and the brain was removed. After fixation using 10% formaldehyde solution, the brain was sectioned in the coronal plane and the ventricle/brain ratio was measured as the

maximum width of ventricle to maximum width of brain. In order to compare the effect of the intrathecal injections, normal mice without any intrathecal injection were used in this study. Body weight and ventricle/brain ratio were measured in the same manner for some normal mice. This animal experiment protocol was approved by the Harvard medical area standing committee on animals and the Beth Israel Deaconess Medical Center Institutional Animal Care & Use Committee.

Results

Body weight of mice

Mean body weight of 12 TGF-β1 injected mice was 22.9±4.72 g. Mean body weight of 16 PBS injected control mice was 20.98±3.17 g. Mean body weight of 23 normal 6-week-old nude mice was 24.27±2.44 g. TGF-β1 injected mice showed significantly lighter body weight than normal mice (Student's t-test, $p<0.05$) and there was no significant difference between TGF-β1 injected mice and PBS injected mice.

The evaluation of the toxicity of the intrathecal injection of ICG-HDL is beyond the scope of this paper. Although we did not experience any acute complications caused by the intrathecal injection of ICG-HDL, a study of the toxicity of intrathecal injection of ICG-HDL should be performed prior to the application of this method in humans.

Ventricle/brain ratio

The fixed brains were sectioned and ventricle/brain ratios were measured. Coronal sectioning was not done appropriately for one mouse in each of the TGF-β1 and PBS injected mouse groups and so these data were omitted from the analysis. Mean ventricle/brain ratio of 11 TGF-β1 injected mice was 0.66±0.11. Mean ventricle/brain ratio of 15 PBS injected control mice was 0.54±0.04. Mean ventricle/brain ratio of 7 normal 6-week-old nude mice was 0.53±0.08. The ventricle/brain ratios of the TGF-β1 injected mice were significantly higher than those of PBS injected (Student's t-test, $p<0.01$) and normal mice (Student's t-test, $p<0.05$). There was no difference between the mean ventricle/brain ratios of control and normal mice.

Serial imaging findings

Figure 1 shows typical images at 4 hours after the injection of ICG-HDL in both control and hydrocephalic mice. The images of control mice show clear ICG accumulation at the cisterna magna and bilateral cerebello-pontine (C-P) angles. Images of hydrocephalus mice demonstrate very limited signal.

As described in a previous paper, we placed regions of interest (ROI) at the cisterna magna and bilateral C-P angle cistern. Full images were not obtained for 5 PBS injected mice, because of anesthetic loss. Figure 2 shows the signal intensity changes within ROIs in the 10 PBS injected mice. The signals from all ROIs exhibited peaks at 4 hours after the injection and decreased

thereafter. Figure 3 showed mean signal intensity changes from ROIs in 11 TGF-β1 injected mice. The signals from all ROIs showed peaks at 4 hours after the injection. All signals decreased thereafter, however the signal from cisterna magna exhibited delayed washout compared to control mice. The TGF-β1 injected mice exhibit lower signal intensity at bilateral C-P angles comparing with control mice, although this is not statistically significant (Student's t-test).

Discussion

Image findings from hydrocephalic mice

Our results indicated that intrathecal injection of TGF-β1 or PBS causes growth retardation and only TGF-β1 injection induced ventricular enlargement. TGF-β1 injected hydrocephalic mice showed diminished CSF movement compared to control mice and our method of imaging CSF flow using NIR fluorescence was sufficient to observe and analyze CSF movement of mice. Moinuddin reported a significant lengthening of the ink passage time and ink stasis in the altered leptomeningeal space in TGF-β1 injected mice [6]. These findings are in agreement with our own. We found no other reports of imaging TGF-β1 injected mice in the literature. In humans, early and persistent ventricular reflux is a typical finding of patients with communicating hydrocephalus [1,7]. In our experiments with mice, no ventricular reflux was observed. Moinuddin also did not report ventricular reflux and stasis [6]. In the

mouse, ventricles are located a few mm below the cerebral surface, so the ventricle is within the range of our imaging technique. We believe that because of remarkable diminution of the CSF flow in hydrocephalic mice, significant amounts of dye didn't enter the ventricles even though there was ventricular reflux. The CSF dynamics might be different between mice and humans. The presence of ventricular reflux in TGF-β1 injected mice might be examined using different dosing or administration methods of TGF-β1.

Mouse hydrocephalus model

There are several methods to induce hydrocephalus in mice. Historically hydrocephalus has been induced by intrathecal injection of silicone oil, kaolin and laminalia [8]. These methods induce severe inflammation at the subarachnoid cistern and cause obstructive hydrocephalus. Milder forms of hydrocephalus have been induced using transgenic mice and fetal exposure to irradiation, drugs or infection [9]. These methods are costly, not efficient and not safe for mice.

There are several rodent models with inherited hydrocephalus. Aqueductal stenosis is a common observation in congenital hydrocephalus and prenatal hydrocephalus has a poor prognosis [10]. The H-Tx rat is a homozygous carrier of an autosomal recessive hydrocephalus gene with incomplete penetrance [10,11]. Most hydrocephalic H-Tx rats die between 4 and 5 weeks of age. Transgenic mice that overexpress TGF-β1 in the central

nervous systems have been reported [12,13]. These mice develop severe hydrocephalus and die between birth and 3 weeks of age [13].

Communicating hydrocephalus is typical mild hydrocephalus in adult human patients after cerebrovascular disease. The malabsorption of CSF is the cause of communicating hydrocephalus and there is no obstruction of CSF flow. As a rodent model of adult human communicating hydrocephalus, the mouse should survive for a prolonged period without severe disability. In our study, communicating hydrocephalus in mice was induced by intrathecal injection of human recombinant TGF-β1. Tada et al. established this method and reported that it was easy, safe and effective [4]. In their experience, all TGF-β1 injected mice showed ventricular dilatation within 3 weeks and survived more than 6 weeks after the injection. This method involves intracerebral injection of TGF-β1, so some brain damage is inevitable. We experienced early death of newborn mice immediately after intracranial injection of TGF-β1. Pathological examination of these 2 dead mice showed intracerebral hemorrhage. A technical refinement of the intracranial injection method such as the use of stereotactic apparatus might prevent some complications. In our experiment, some mice did not survive 4 weeks post injection, however, all TGF-β1 injected mice that survived for 4 weeks showed ventricular dilatation. The degree of ventricular dilatation was quite variable as Tada has reported.

TGF-β1

TGF-β1 is a dimmer of a 25-kDa polypeptide. TGF-β has been isolated as the protein to induce a transformed phenotype in rat fibroblasts [14]. In the developing central nervous system, the presence of TGF-β1 and expression of TGF-β1 receptors occur preferentially in meninges and the subarachnoid space in both hydrocephalic and normal mice [15]. Activated T lymphocytes secrete greatly elevated levels of TGF-β, so TGF-β is one of the lymphokines produced by T lymphocytes [16]. TGF-β1 is chemotactic to monocytes and fibroblasts and enhances angiogenesis and formation of extracellular matrix proteins such as collagen and fibronectin [17]. In addition, TGF-β1 is known to cause formation of granulation tissue, fibrosis in wound healing, certain fibrotic diseases such as liver cirrhosis, pulmonary fibrosis and glomerulonephritis [16,18]. Kitazawa found elevated levels of TGF-β1 in the CSF of patients with hydrocephalus after subarachnoid hemorrhage [19]. TGF-β1 injected mice showed inter-meningeal fibrosis and a subsequent narrowing of the intrameningeal CSF space [6,20]. We believe that the consequence of intracranial injection of TGF-β1 is a good model of communicating hydrocephalus because it has the same pathophysiology as human hydrocephalus after subarachnoid hemorrhage. Optimizing the dose, timing and delivery method might make this model more efficient and convenient.

We can induce communicating hydrocephalus model in nude mice via intrathecal injection of TGF-β1. Nude mice do not have mature T lymphocytes [21]. These findings reveal therefore that the induction of hydrocephalus using TGF-β1 doesn't require mature T lymphocytes. This means that subarachnoid fibrosis induced by TGF-β1 results from a direct proliferative response rather than indirect chemotactic actions or immune responses. In addition, TGF-β1 is immunosuppressive in vivo and depresses the number and activity of natural killer cells [22,23]. Leukocytes from nude mice produced less active TGF-β1 than those from normal mice [23]. These findings support the mechanism of subarachnoid fibrosis induced by TGF-β1, that is the direct formation of extracellular matrix proteins by fibroblasts.

Advantage and limitation of optical imaging

The advantages of optical imaging are noninvasiveness except for the injection of a fluorescent probe and rapid and repeatable image acquisition. The imaging system is compact and portable, so that intraoperative and bedside applications could be possible. The disadvantages are the reduction in image quality due to the photon scattering and the limitation of signal acquisition from deep tissue. Our study clarified the usefulness of this technique for CSF flow imaging in nude mice. The application of this methodology in human CSF flow imaging would be challenging without future technical innovations.

Legends of figures

Fig. 1 Typical images at 4 hours after the injection of ICG-HDL in both hydrocephalus and control mice

Fig. 2 Mean signal intensity over time from ROIs located over brain regions in 10 PBS injected control mice

Fig. 3 Mean signal intensity over time from ROIs located over brain regions in 11 TGF−β1 injected hydrocephalus mice

Figure 1

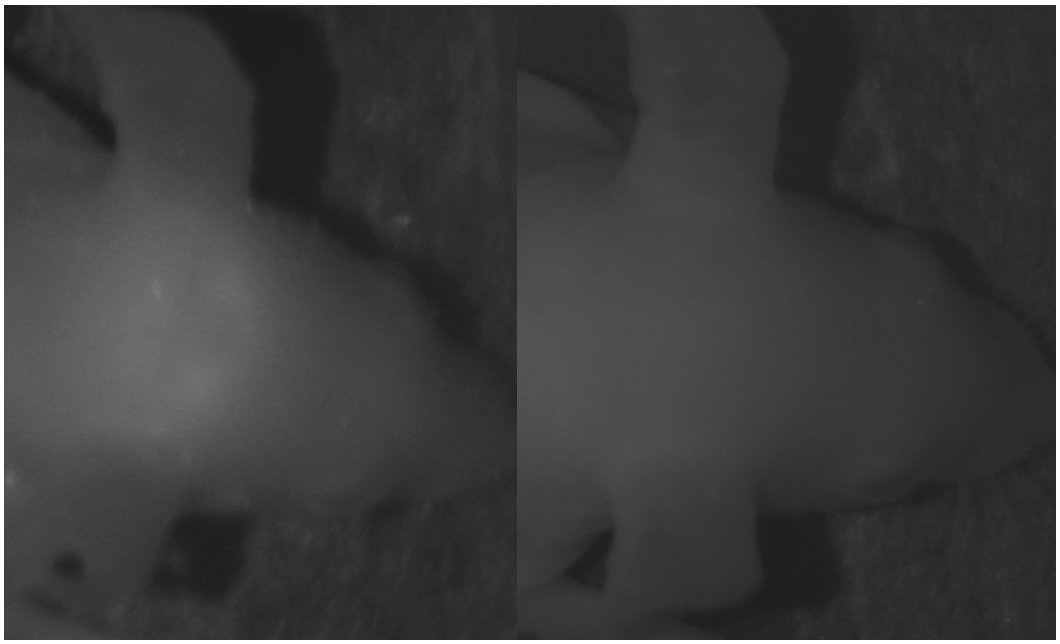

control mouse hydrocephalic mouse

Figure 2

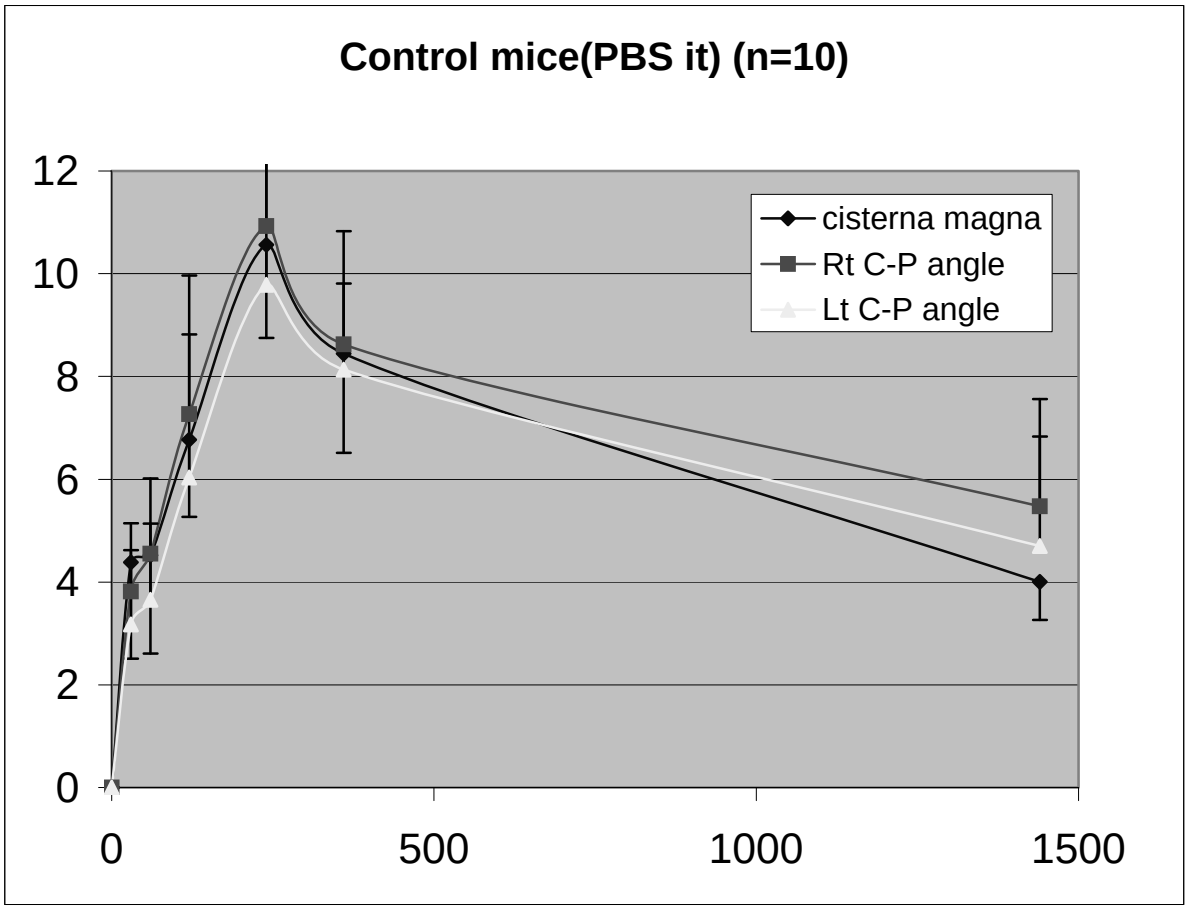
Control mice(PBS it) (n=10)
12
10
8
6
4
2
0
0
500
1000
1500
cisterna magna
Rt C-P angle
Lt C-P angle

Figure 3

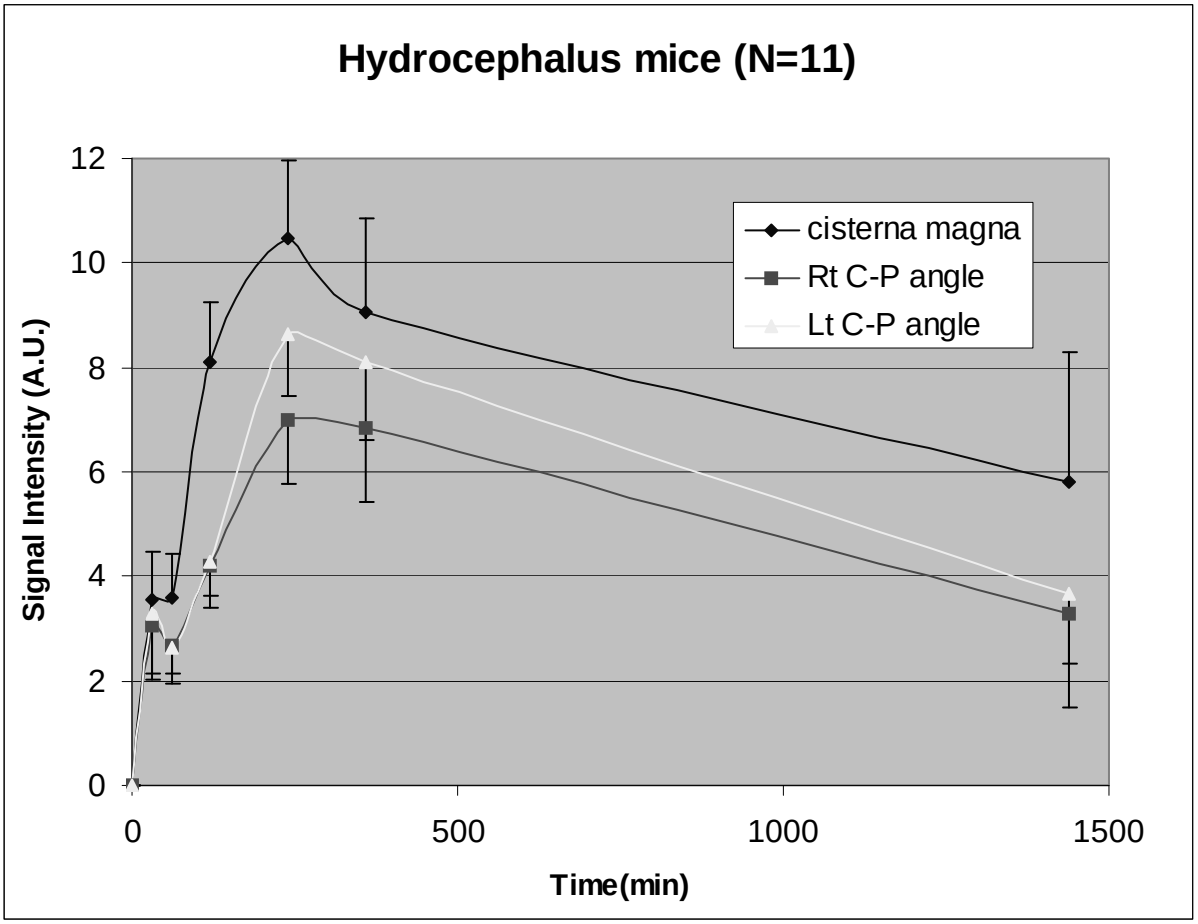
Hydrocephalus mice (N=11)
Signal Intensity (A.U.)
Time(min)
cisterna magna
Rt C-P angle
Lt C-P angle
0
2
4
6
8
10
12
0
500
1000
1500

References

[1] Drayer BP, Rosenbaum AE (1978) Studies of the third circulation. Amipaque CT cisternography and ventriculography, J Neurosurg 48:946-956

[2] Kim MH, Shin KM, Song JH (1998) Cine MR CSF flow study in hydrocephalus: what are the valuable parameter? Acta Neurochir Suppl(Wien) 71:343-346

[3] Shibata Y, Kruskal JB, Palmer MP (2005) Imaging of cerebrospinal fluid space and movement in mice using near infrared fluorescence. J Neuroscience Methods 147:82-87

[4] Tada T, Kanaji, M, Kobayashi S (1994) Induction of communicating hydrocephalus in mice by intrathecal injection of human recombinant transforming growth factor-beta 1. J Neuroimmunol 501:53-158

[5] Baker KJ (1966) Binding of sulfobromophthalein (BSP) sodium and indocyanine green (ICG) by plasma alpha-1 lipoproteins, Proc Soc Exp Biol Med 122:957-963

[6] Moinuddin SM, Tada T (2000) Study of cerebrospinal fluid flow dynamics in TGF-beta 1 induced chronic hydrocephalic mice. Neurol Res 22:215-222

[7] Tamaki N, Kanazawa Y, Asada M, Kusunoki T, Matsumoto S (1979) Dynamics of cerebrospinal fluid circulation evaluated by metrizamide CT cisternography. J Comput Assist Tomogr 3:209-216

[8] Matsumoto S, Hirayama A, Yamasaki S, Shirataki K, Fujiwara K (1975) Comparative study of various models of experimental hydrocephalus. Childs Brain 1:236-242

[9] Aolad HM, Inouye M, Hayasaka S, Darmanto W, Murata Y (1998) Congenital hydrocephalus caused by exposure to low level X-radiation at early gestational stage in mice. Biol Sci Space 12:256-257

[10] Jones HC, Lopman BA, Jones TW, Carter BJ, Depelteau JS, Morel L (2000) The expression of inherited hydrocephalus in H-Tx rats. Childs Nerv Syst 16:578-584

[11] Cai X, McGraw G, Pattisapu JV, von Kalm L, Willingham S, Socci D et al. (2000) Hydrocephalus in the H-Tx Rat: A Monogenic Disease? Experimental Neurology 163:131-135

[12] Hayashi N, Leifer DW, Cohen AR (2000) Chronologic changes of cerebral ventricular size in a transgenic model of hydrocephalus. Pediatr Neurosurg 33:182-187

[13] Galbreath E, Kim SJ, Park K, Brenner M, Messing A (1995) Overexpression of TGF-beta 1 in the central nervous system of transgenic mice results in hydrocephalus. J Neuropathol Exp Neurol 54:339-349

[14] Roberts AB, Anzano MA, Lamb LC, Smith JM, Sporn MB (1981) New class of transforming growth factors potentiated by epidermal growth factor: isolation from non-neoplastic tissues. Proc Natl Acad Sci USA 78:5339-5343

[15] Cohen AR, Leifer DW, Zechel M, Flaningan DP, Lewin JS, Lust WD (1999) Characterization of a model of hydrocephalus in transgenic mice. J Neurosurg 91:978-988

[16] Roberts AB, Sporn MB, Assoian RK, Smith JM, Roche NS, Wakefield LM, et al. (1986) Transforming growth factor type beta: rapid induction of fibrosis and angiogenesis in vivo and stimulation of collagen formation in vitro. Proc Natl Acad Sci USA 83:4167-4171

[17] Ignotz RA, Massague J (1986) Transforming growth factor-beta stimulates the expression of fibronectin and collagen and their incorporation into the extracellular matrix. J Biol Chem 261:4337-4345

[18] Massague J (1990) The transforming growth factor-beta family. Annu Rev Cell Biol 6:597-641

[19] Kitazawa K, Tada T (1994) Elevation of transforming growth factor-beta 1 level in cerebrospinal fluid of patients with communicating hydrocephalus after subarachnoid hemorrhage, Stroke 25:1400-1404

[20] Nitta J, Tada T (1998) Ultramicroscopic structures of the leptomeninx of mice with communicating hydrocephalus induced by human recombinant transforming growth factor-beta 1. Neurol Med Chir (Tokyo) 38:819-824

[21] Pelleitier M, Montplaisir S (1975) The nude mouse: a model of deficient T-cell function. Methods Achiev Exp Pathol 7:149-166

[22] Wallick SC, Figari IS, Morris RE, Levinson AD, Palladino MA (1990) Immunoregulatory role of transforming growth factor beta (TGF-beta) in development of killer cells: comparison of active and latent TGF-beta 1. J Exp Med 172:1777-1784

[23] Su HC, Ishikawa R, Biron CA (1993) Transforming growth factor-beta expression and natural killer cell responses during virus infection of normal, nude, and SCID mice. J Immunol 151:4874-4890